Chromatic aberration correction of the human eye for retinal imaging in the near infrared

Enrique J. Fernández

Center for Biomedical Engineering and Physics, Medical University of Vienna, Austria
Laboratorio de Optica, Departamento de Física, Universidad de Murcia, Campus de Espinardo (Ed. C), 30071 Murcia, Spain
enrique.fernandez@meduniwien.ac.at

Angelika Unterhuber, Boris Považay, Boris Hermann

Center for Biomedical Engineering and Physics, Medical University of Vienna, Austria
angelika.unterhuber@meduniwien.ac.at, boris.povazay@meduniwien.ac.at, boris.hermann@meduniwien.ac.at

Pablo Artal

Laboratorio de Optica, Departamento de Física,Universidad de Murcia, Campus de Espinardo (Ed. C), 30071 Murcia, Spain
pablo@um.es

Wolfgang Drexler

Center for Biomedical Engineering and Physics, Medical University of Vienna, Austria
wolfgang.drexler@meduniwien.ac.at

Abstract: An achromatizing lens has been designed for the human eye in the near infrared range, from 700 to 900 nm, for retinal imaging purposes. Analysis of the performance of the lens, including tolerance to misalignments, has been mathematically accomplished by using an existing eye model. The calculations have shown a virtually perfect correction of the ocular longitudinal chromatic aberration, while still keeping a high optical quality. Ocular aberrations in five subjects have been measured with and without the achromatizing lens by using a Hartmann-Shack wavefront sensor and a broad bandwidth femtosecond Ti:sapphire laser in the spectral range of interest with a set of interference filters, studying the benefits and limits in the use of the achromatizing lens. Ocular longitudinal chromatic aberration has been experimentally demonstrated to be fully corrected by the proposed lens, with no induction of any other parasitic aberration. The practical implementation of the achromatizing lens for Ophthalmoscopy, specifically for optical coherence tomography where the use of polychromatic light sources in the near infrared portion of the spectrum is mandatory, has been considered. The potential benefits of using this lens in combination with adaptive optics to achieve a full aberration correction of the human eye for retinal imaging have also been discussed.

OCIS codes: (220.1000) Aberration compensation; (330.4460) Ophthalmic optics; (330.5370) Physiological optics; (170.4500) Optical coherence tomography; (010.1080) Adaptive optics.

References and links

1. J. G. Sivak and T. Mandelman, "Chromatic dispersion of the ocular media," Vision Res. **16**, 997-1003 (1982).
2. P. A. Howarth, "The lateral chromatic aberration of the eye," Ophthalmol. Physiol. Opt. **4**, 223-226 (1984).
3. L. N. Thibos, "Calculation of the influence of lateral chromatic aberration on image quality across the visual field," J. Opt. Soc. Am. A **4**, 1673-1680 (1987).
4. Y. U. Ogboso and H. E. Bedell, "Magnitude of lateral chromatic aberration across the retina of the human

#69489 - $15.00 USD Received 30 March 2006; revised 14 June 2006; accepted 19 June 2006

eye," J. Opt. Soc. Am. A **4**, 1666-1672 (1987).
5. I. Newton, *Opticks* (1730), fourth edition, Book I, Part 2, Prop. VIII. (Reprinted by Bell, London, 1931).
6. T. Young, "An account of some cases of the production of colors, not hitherto described," Phil. Trans. Roy. Soc. London **92**, 387-397 (1802).
7. J. Fraunhofer, "Bestimmung des Brechungs- und des Farbenzerstreuungs-Vermbgens verschiedener Glasarten, in Bezug auf die Vervollkommnung achromatischer Fernröhre," Ann. d. Physik (Gilbert) **56**, 264-313 (1817).
8. A. Matthiessen, "Determination exacte de la dispersion de l'oeil humain, par des mesures directes," Comptes rendus Acad. Sci., Paris **24**, 875 (1847).
9. H. von Helmholtz, *Treatise on Physiological Optics* (1866); translation from third German edition (1909) ed. by Southall, Opt. Soc. Am. Vol. I (1924).
10. G. Wald and D. T. Griffin, "The change in refractive power of the human eye in dim and bright light," J. Opt. Soc. Am. **37**, 321-329 (1947).
11. A. Ivanoff, *Les aberrations de l'Oeil*, (Mason, Paris, 1953).
12. R. E. Bedford and G. Wyszecki, "Axial chromatic aberration of the human eye," J. Opt. Soc. Am. **47**, 564-565 (1957).
13. M. Millodot and J. G. Sivak, "Influence of accommodation on the chromatic aberration of the eye," Br. J. Physiol. Opt. **28**, 169-174 (1973).
14. W. N. Charman and J. A. M. Jennings, "Objective measurements of the longitudinal chromatic aberration the human eye," Vision Res. **16**, 99-105 (1976).
15. P. A. Howarth and A. Bradley, "The longitudinal chromatic aberration of the eye and its correction," Vision Res. **26**, 361-366 (1986).
16. D. P. Cooper and P. L. Pease, "Longitudinal chromatic aberration of the human eye and wavelength in focus," Am. J. Optom. Physiol. Opt. **65**, 99-107 (1988).
17. L. N. Thibos, A. Bradley, and X. Zhang, "The effect of ocular chromatic aberration on monocular visual performance," Optom. Vision Sci. **68**, 599-607 (1991).
18. C. Ware, "Human axial chromatic aberration found not to decline with age," A. Graefes Arch. Klin. Exper. Ophthalmol. **218**, 39-41 (1982).
19. P. A. Howarth, X. X. Zhang, A. Bradley, D. L. Still, and L. N. Thibos, "Does the chromatic aberration of the eye vary with age?," J. Opt. Soc. Am. A **5**, 2087-2092 (1988).
20. M. C. Rynders, R. Navarro, and M. A. Losada, "Objective measurement of the off-axis longitudinal chromatic aberration in the human eye," Vision Res. **37**, 513-521 (1997).
21. J. Porter, A. Guirao, I. G. Cox, and D. R. Williams, "Monochromatic aberrations of the human eye in a large population," J. Opt. Soc. Am. A **18**, 1793–1803 (2001).
22. L. N. Thibos, X. Hong, A. Bradley, and X. Cheng, "Statistical variation of aberration structure and image quality in a normal population of healthy eyes," J. Opt. Soc. Am. A **19**, 2329-2348 (2002).
23. F. Castejón-Mochón, N. López-Gil, A. Benito, P. Artal, "Ocular wave-front statistics in a normal young population," Vision Res. **42**, 1611-1617 (2002).
24. P. Artal, E. Berrio, A. Guirao, and P. Piers, "Contribution of the cornea and internal surfaces to the change of ocular aberrations with age," J. Opt. Soc. Am. A **19**, 137-143 (2002).
25. E. J. Fernández, A. Unterhuber, P. M. Prieto, B. Hermann, W. Drexler, and P. Artal, "Ocular aberrations as a function of wavelength in the near infrared measured with a femtosecond laser," Opt. Express **13**, 400-409 (2005).
26. D. A. Atchinson and G. Smith, "Chromatic dispersions of the ocular media of human eyes," J. Opt. Soc. Am. A **22**, 29-36 (2005).
27. A. C. van Heel, "Correcting the spherical and chromatic aberrations of the eye," J. Opt. Soc. Am. **36**, 237-239 (1947).
28. A. Ames and C. A. Proctor, "Dioptrics of the eye," J. Opt. Soc. Am. **5**, 22-84 (1921).
29. A. L. Lewis, M. Katz, and C. Oehrlein, "A modified achromatizing lens," Am. J. Optom. Physiol. Opt. **59**, 909-911 (1982).
30. I. Powell, "Lenses for correcting chromatic aberration of the eye," App. Opt. **20**, 4152-4155 (1981).
31. F. C. Delory and K. P. Plibsen, "Spectral reflectance of the human ocular fundus," App. Opt. **28**, 1061-1067 (1989).
32. D. Huang, E. A. Swanson, C. P. Lin, J. S. Schuman,W. G. Stinson, W. Chang, M. R. Hee, T. Flotte, K. Gregory, C. A. Puliafito, and J. G. Fujimoto, "Optical coherence tomography," Science **254**, 1178-1181 (1991).
33. T. Fuji, A. Unterhuber, V. S. Yakolev, G. Tempea, A. Stingl, F. Krausz, and W. Drexler, "Generation of smooth, ultra-broadband spectral directly from a prism-less Ti:sapphire laser," Appl. Phys. B **77**, 125-128 (2003).
34. W. Drexler, U. Morgner, R. K. Ghanta, F. X. Kärtner, J. S. Schuman, and J. G. Fujimoto, "Ultrahighresolution ophthalmic optical coherence tomography," Nature Medicine **7**, 502-507 (2001).
35. Y. Zhang, J. Rha, R.S. Jonnal, D.T. Miller, "Adaptive optics parallel spectral domain optical coherence tomography for imaging the living retina," Opt. Express **13**, 4792-4811 (2005).
36. R. Zawadzki, S. Jones, S. Olivier, M. Zhao, B. Bower, J. Izatt, S. Choi, S. Laut, and J. Werner, "Adaptive-

#69489 - $15.00 USD Received 30 March 2006; revised 14 June 2006; accepted 19 June 2006

optics optical coherence tomography for high-resolution and high-speed 3D retinal in vivo imaging," Opt. Express **13**, 8532-8546 (2005).
37. B. Hermann, E.J. Fernández, A. Unterhuber, H. Sattmann, A.F. Fercher, and W. Drexler, P.M. Prieto and P. Artal, "Adaptive-optics ultrahigh-resolution optical coherence tomography," Opt. Lett. **29**, 2142-2144 (2004).
38. E. J. Fernández, B. Povazay, B. Hermann, A. Unterhuber, H. Sattmann, P. M. Prieto, R. Leitgeb, P. Ahnelt, P. Artal, and W. Drexler, "Three dimensional adaptive optics ultrahigh-resolution optical coherence tomography using a liquid crystal spatial light modulator," Vision Res. **45**, 3432-3444 (2005).
39. E. J. Fernández and W. Drexler, "Influence of ocular chromatic aberration and pupil size on transverse resolution in ophthalmic adaptive optics optical coherence tomography," Opt. Express **13**, 8184-8197 (2005).
40. A. Gullstrand, Appendix II in *Handbuch der Physiologischen Optik*, H. von Helmholtz, ed., 3rd ed. (Voss, Hamburg, 1909).
41. Y. Le Grand and S. G. El Hage, *Physiological Optics* (Springer-Verlag, Berlin, 1980).
42. L. N. Thibos, M. Ye, X. Zhang, and A. Bradley, "Spherical aberration of the reduced schematic eye with elliptical refracting surface," Optom. Vision Sci. **74**, 548–556 (1997).
43. O. Pomerantzeff, M. Pankratov, G.-J. Wang, and P. Dufault, "Wide-angle optical model of the eye," Am. J. Optom. Physiol. Opt. **61**, 166–176 (1984).
44. H.-L. Liou and N. A. Brennan, "Anatomically accurate, finite model eye for optical modeling," J. Opt. Soc. Am. A **14**, 1684–1695 (1997).
45. D. A. Atchison and G. Smith, "Continuous gradient index and shell models of the human lens," Vision Res. **35**, 2529–2538 (1995).
46. R. Navarro, J. Santamaría, and J. Bescós, "Accommodation-dependent model of the human eye with aspherics," J. Opt. Soc. Am. A **2**, 1273-1281 (1985).
47. W. Lotmar, "Theoretical eye model with aspherics," J. Opt. Soc. Am. **61**, 1522–1529 (1971).
48. I. Escudero-Sanz and R. Navarro, "Off-axis aberrations of wide-angle schematic eye model," J. Opt. Soc Am. A **16**, 1881-1891 (1999).
49. E. J. Fernández, A. Unterhuber, P. M. Prieto, B. Hermann, W. Drexler, and P. Artal, "Near infrared ocular wavefront sensing with a femtosecond laser," ARVO abstract **2836** (2004).
50. P. M. Prieto, F. Vargas-Martín, S. Goelz, and P. Artal, "Analysis of the performance of the Hartmann-Shack sensor in the human eye," J. Opt. Soc. Am. A **17**, 1388-1398 (2000).
51. American National Standard Institute, *American National Standard for Safe Use of Lasers*, ANSI Z 136-1 (2000).

1. Introduction

The human eye's optical media exhibit significant chromatic dispersion [1] caused by their wavelength dependent refractive indices. In order to simplify the study of ocular chromatic aberration it is common practice to separate the effects in longitudinal or axial chromatic aberration (LCA), and in transverse or lateral chromatic aberration (TCA). LCA manifests as a change in the focusing plane as a function of the wavelength and is also referred to as chromatic defocus or axial color. TCA appears with off-axis illumination and leads to a transversal shift of focus for different wavelengths. As a consequence, due to TCA the effective magnification is wavelength dependent [2-4]. Therefore, this lateral or transversal aberration is typically associated with extended objects.

LCA in the eye was first mentioned by Newton (1730) [5]. Many other historical opticians also studied this aberration in the context of the Physiological Optics, as Young [6], Fraunhofer [7], Matthiessen [8] and Helmholtz [9]. A number of measurements of the LCA have been reported in the last century, by using many different objective and subjective methods in the visible range [10-17]. The magnitude of the LCA is ~ 2.5 D from 400 to 700 nm. LCA is known to be similar among different eyes, and essentially independent of age [16,18,19]. LCA is also practically invariant as a function of field, for small and moderate ranges [20]. Therefore, ocular LCA can be assumed to be constant for a given spectral range, in particular as compared to monochromatic aberrations, which present a much larger variability among subjects [21-23] and age [24]. Only recently, the LCA of the eye has been systematically obtained [25] and mathematically modeled in the near infrared (NIR) portion of the spectrum [26]. Between 700 and 900 nm the value of the ocular LCA is ~ 0.4 D.

#69489 - $15.00 USD Received 30 March 2006; revised 14 June 2006; accepted 19 June 2006

Achromatizing the human eye by using refractive elements has been accomplished in the past in the visible range, exclusively for visual applications. Different lens designs have been proposed for this purpose. In this context, van Heel first presented a symmetrical triplet [27], based on experimental measurements of LCA accomplished by Ames and Proctor in only 3 subjects [28], reporting a subjective gain in vision when employing such a lens with polychromatic stimulus. The idea of a symmetrical triplet was also exploited by Bedford and Wyszecki [12]. The last achromatizing lens (AL) reported for the visible based on a triplet design was developed by Lewis and collaborators [29]. All of these mentioned lenses suffered from a rapid increase in TCA off-axis. In order to overcome this fundamental limitation, particularly important when testing the lenses with extended polychromatic objects, Powel proposed the use of a more complex design to achromatize the eye, compounded by a triplet and a doublet air-spaced [30].

All these previous designs were intended to enhance vision, by introducing the opposite LCA found in the human eye. ALs have been never proposed for retinal imaging, and different spectral ranges than the visible have never been considered. A fundamental reason for such a lack of interest in other applications has been the extended use of monochromatic or quasi-monochromatic light sources in Ophthalmoscopy. In addition, modern ophthalmoscopes preferably use infrared light, increasing the amount of light reflected or back-scattered from the retina [31], having been only very recently characterized the associated LCA in this spectral range [25].

Nevertheless, a relatively new ophthalmic imaging modality has been developed in recent years, where the use of polychromatic light sources is absolutely mandatory: optical coherence tomography (OCT). This non-invasive ophthalmic technique is based on white light interferometry [32]. In OCT axial resolution is governed by the spectral bandwidth of the light source. The use of broad bandwidth pulsed lasers, emitting continuous Gaussian spectra in the NIR of 130 nm FWHM [33], has enabled up to 2-3 μm of axial resolution in the living retina in ultrahigh resolution (UHR) OCT [34]. In both standard, by using light sources of ~ 50 nm FWHM spectral bandwidth, and UHR OCT, transverse resolution however remains in the order of 20 μm. In order to increase transverse resolution in this ophthalmic modality, the expansion of pupils and beams in the system with the simultaneous use of adaptive optics to compensate the monochromatic aberrations of the eye has been proposed and demonstrated, in both standard OCT [35,36] and in UHR OCT [37,38]. In this context an interesting paradox has recently been reported: when correcting monochromatic aberration through a 6 mm pupil size, Fernández and collaborators did not find any increase in the signal-to-noise ratio of the acquired retinal images as compared to the uncorrected case [38]. Following this work, Fernández and Drexler [39] mathematically studied the influence of chromatic aberration in OCT, finding that ocular LCA might reduce the amount of light received at the detector, and consequently the SNR of the corresponding retinal images, up to 60 % when using light sources centered at 800 nm and 130 nm FWHM, the case of UHR OCT.

Therefore, the correction of the LCA in OCT could be required to further improve the quality of the retinal images, especially when large pupils and broad bandwidth spectra are used. In the current work we investigate the correction of the ocular LCA in the NIR for retinal imaging. We demonstrate the design and performance of an AL and discuss its possible practical implementation.

2. Methods

2.1. Design of the achromatizing lens

A number of mathematical eye models are available in the literature with diverse degrees of complexity [40-47], although none of those has been designed for spectral ranges different than for the visible (from 400 to 700 nm). In the present work, the model proposed by Navarro and collaborators [46] was selected in order to design an AL for the NIR. This eye model is similar to the Gullstrand-Le Grand eye [41], but aspheric surfaces are used instead for the surface of the anterior cornea and crystalline lens in order to better match experimental data

#69489 - $15.00 USD Received 30 March 2006; revised 14 June 2006; accepted 19 June 2006

from real eyes. Radius of curvature of the anterior surface of the cornea and its refractive index are also slightly different in Navarro's eye model as compared to Gullstrand-Le Grand eye. Navarro's model, with small modifications, has also been demonstrated for studying off-axis aberrations, including those associated to wide-angle illumination, by considering the retinal plane as a spherical surface [48]. LCA predicted by this model was compared with experimental data from real eyes obtained in the visible range [10,11], showing very high agreement [46]. Recently, Atchinson and Smith [26] have extended Navarro's model to the NIR by using experimental data from real eyes obtained by Fernández and collaborators [25,49], who first proposed a simple linear equation to model ocular LCA in the NIR.

For the practical design and analysis of the performance of the lens we used Zemax, a commercial program for optical design.

As a first step, several commercially available optical glasses were selected, ignoring those with high cost or difficult to acquire. The search of the optimum geometrical parameters of the lens was done with the help of Zemax, playing with different combinations of optical glasses. The merit functions selected to be minimized by the optimization algorithm were the LCA, the total thickness of the lens and the size of the final point image through the system, in order to obtain a triplet with an acceptable optical quality. The program accepts modulation factors for every merit function. This way allows the user to establish and play with different levels of priorities for the selected functions. In all the optimization processes, the correction of the LCA was set to the maximum priority. For every given pair of optical glasses, the degrees of freedom during the optimization process were the radii of curvature of the different refractive surfaces and their thicknesses. The lens was also constrained to be symmetrical.

2.2. Experimental setup for testing the lens

A relatively simple optical system, depicted in Fig. 1, was implemented to measure the effect of the AL on the human eye. The apparatus incorporated a Hartmann-Shack wavefront sensor [50], allowing the objective estimation of the aberrations with and without the AL. The system conjugated the entrance pupil of the eye, the AL and the Hartmann-Shack sensor by means of two telescopes. The wavefront sensor used a CCD camera with quantum efficiency optimized for the NIR (Hamamatsu C7555) and an array of square microlenses, 0.3 mm size and 7.6 mm focal length, mounted on the camera. Since the AL was designed to exactly compensate for the LCA of the eye, absolute magnification of 1 is required between the eye's entrance pupil and the AL, yielding that the two first lenses of the system, both labeled in Fig. 1 as L1 (f_1' = 150 mm), have to be necessarily identical (in this case magnification -1 is obtained). It has to be said that locating the AL directly in front of the eye is also possible, although perfect conjugation with the eye's pupil is then not possible and alignment during the measurements is more complicated due to the other optical elements. The second telescope, formed by L1 and L2 (f_2' = 100), comprised the pupil size to match the appropriate diameter at the wavefront sensor. All the lenses implemented in the set-up were off-the-shell achromatic doublets designed for the NIR. Subjects were fixed by using a bite-bar, with the mold of the dental impression clamped to a 3-D positioning system. In order to assure an optimum alignment of the AL respect to the rest of the system, the lens was mounted on a special holder allowing micrometric control of tilts as well as movements in the XY plane (perpendicular to the direction of the incoming light).

#69489 - $15.00 USD Received 30 March 2006; revised 14 June 2006; accepted 19 June 2006

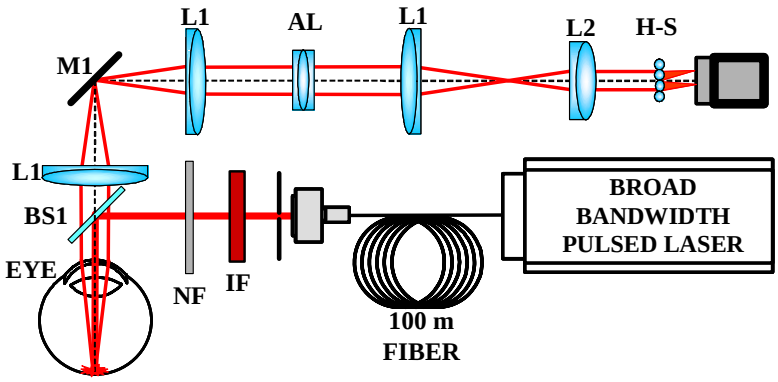

Fig. 1. Experimental setup for testing the effect of the achromatizing lens (AL) on the human eye. The apparatus uses a broad bandwidth pulsed laser emitting in the NIR and a Hartmann-Shack (H-S) wavefront sensor. The eye's entrance pupil and the AL are optically conjugated in the system. NF and IF are neutral and interference filters, respectively.

A compact sub 10 femtosecond Ti:sapphire laser with a center wavelength of 800 nm and up to 160 nm FWHM optical bandwidth with 400 mW output power was employed for this experiment. Because the laser source generates femtosecond pulses, light emitted by the broad bandwidth laser was launched into a 100 meter long monomode optical fiber which was used to provide dispersive stretching of the pulse duration to hundreds of picoseconds. This reduces the peak pulse intensities by several orders of magnitude and since the laser operates at a 75 MHz repetition rate, the output can be treated as continuous wave. An achromatic lens collimated the beam out of the fiber. A movable stop was used to displace the 1 mm entrance beam from the corneal apex, minimizing reflections. A set of interference filters (each of 10 nm bandwidth, indicated in Fig. 1 as IF) were used to select different wavelengths within the range of interest: 700, 730, 750, 780, 800, 850, 870 and 900 nm. A neutral filter (NF in Fig. 1) was also located in the illuminating arm to adjust the flux intensity finally sent to the eye. Intensity was always kept under 15 $\mu W/cm^2$, near to 2 orders of magnitude below the maximum exposure limit for the retina [51]. Five subjects, familiar with the purpose of the experiment, with ages ranging from 29 to 39 (Mean = 32.2 years, s.d. = 4) participated in the measurements. In order to minimize changes in accommodation, affecting the subsequent estimation of the LCA through the defocus, cyclopentolate (0.5 %) was instilled in the eye (left eye was systematically selected) of the subjects immediately before the measurements. Fixation target was not used during the measurements. Ocular aberrations were recorded in 2 different runs, each of them at 30 Hz during 2 seconds for every subject. The procedure was repeated for each interference filter, with and without the AL implemented in the system. The filters were randomly implemented for every subject, avoiding any established order. Subjects were allowed to leave the bite-bar between runs. The experimental procedure was similar to the one reported by Fernández and collaborators to measure the ocular LCA in the NIR [25].

3. Results

3.1. Achromatizing lens

Figure 2 depicts the AL proposed for the human eye in the NIR. The lens is a triplet made of common materials (F2 and N-SK4, Schott catalogue) with a symmetric design, resulting in a cost-effective lens. The triplet was manufactured by Linos Photonics, Inc.. The diameter of the lens was 12.7 mm, being easy to mount in standard holders.

The right side of Fig. 2 shows the chromatic focal shift at the retina estimated by the optical design program for the eye model (in blue color, labeled as natural eye) and also for the combination of lens and eye (in red color). The focal shift caused by 1 D in our eye model,

#69489 - $15.00 USD Received 30 March 2006; revised 14 June 2006; accepted 19 June 2006

using a pupil of 6 mm diameter and 800 nm wavelength, is 381.19 μm. The dashed line indicates the perfect case, with no focal shift at the retinal plane. According to this figure, the proposed lens fully corrects LCA in the selected spectral range.

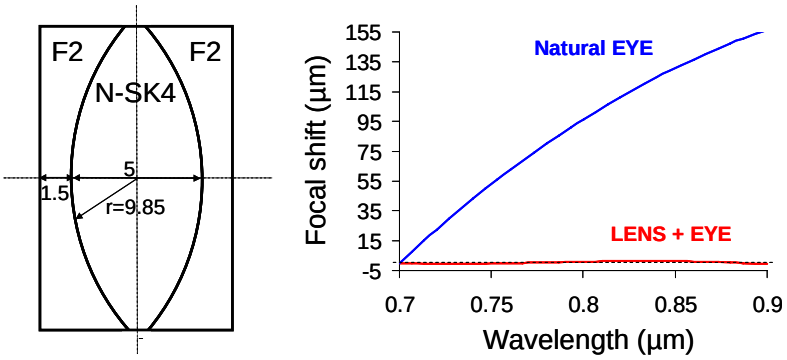

Fig. 2. Left: Achromatizing lens (AL) design. All dimensions are given in mm. Right: Chromatic focal shift at the retina for the eye model (see text for more details) in the NIR (in blue color) and for the combination of the eye model and the AL (in red). The dashed line indicates the zero chromatic shift.

To emulate the actual behavior in real eyes, chromatic focal shift was obtained in the program by using a pupil of 6 mm diameter. A homogeneous distribution of rays covering the whole pupil, consequently marginal rays were also considered, were used for calculations. Geometrical point spread functions (PSFs) at different wavelengths are presented in Fig. 3, showing the effect of the AL on the images projected on the retina. All images are obtained at the plane where wavelength 800 nm is focused. In the eye model, PSFs exhibit a noticeable change as a function of wavelength, while the use of the AL forces the different PSFs to be virtually identical. This fact can be even better appreciated at the bottom of the figure, where the polychromatic PSFs in the corrected and natural cases are depicted for several wavelengths.

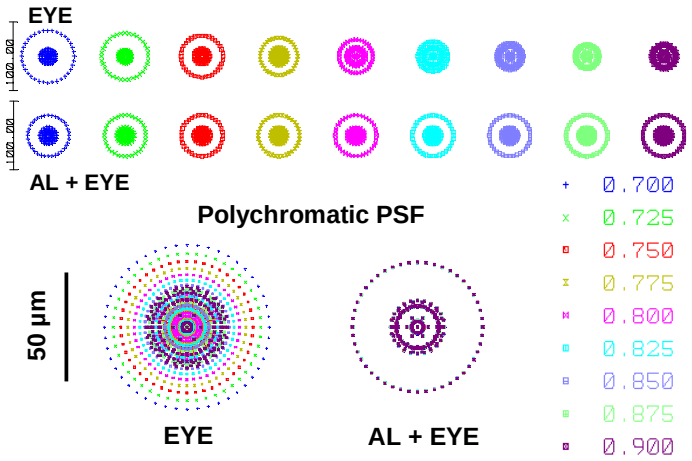

Fig. 3. Geometrical point spread functions (PSFs) of the eye model calculated without and with the achromatizing lens through a 6 mm pupil with marginal rays for several wavelengths, presented with different colors. The polychromatic PSFs in both situations are showed at the bottom.

#69489 - $15.00 USD Received 30 March 2006; revised 14 June 2006; accepted 19 June 2006

In practice, the AL can only be approximately aligned respecting the eye's entrance pupil. Moreover, a hypothetical perfect alignment with the entrance pupil would not assure that the optical axes of the eye and lens are coincident, not even parallel to each other. Therefore it is useful to analyze the performance of the AL in presence of tilts and misalignments, covering realistic ranges. This is particularly important for the case of NIR illumination, where subjective alignment can not be performed by the subject. Although the human retina is still active in the range of 700 to 900 nm, subjects perceive the light from different wavelengths in this portion of the spectrum as a single color (red), only distinguishing changes in the intensity. Figure 4 shows the results of the performance of the lens with the eye model at different situations (calculated through a pupil of 6 mm and using marginal rays). The first column of Fig. 4 presents the results from the simulations obtained for the case of pure tilt around the X axis. Tilts in the Y axis must produce similar results due to the symmetry of the problem. A schematic depicts the modeled tilt. Defocus, calculated at the exit pupil of the eye model, is obtained from the Zernike polynomials coefficients, taking into account those terms with square dependence of the radial coordinate. The change of defocus at any wavelength in the considered NIR range as a function of the tilt is presented at the top of Fig. 4. The simulation covered up to 12 degrees of tilt, which was clearly including both the values one should expect after a careful alignment of the optical system and the reasonable changes in the position of the eye when using a bite-bar to stabilize the subject. The figure shows that defocus monotonically increases with the induced tilt. For tilts of 12 degrees the defocus error is larger than 0.12 D. The main cause of the change in defocus is the total thickness of the AL. Since the experimental protocol in the real measurements allowed subjects to rest between consecutive runs, this source of variation could potentially play a role in the obtained LCA. At the bottom of the figure the lateral color is presented as a function of the tilt. Lateral color was obtained as the distance (in μm) between the marginal rays of the two extreme wavelengths of the considered range (900 and 700 nm) at the retinal plane. The curve shows in this case a modest effect over the lateral color, barely surpassing the size of the diffraction image (~ 5 μm).

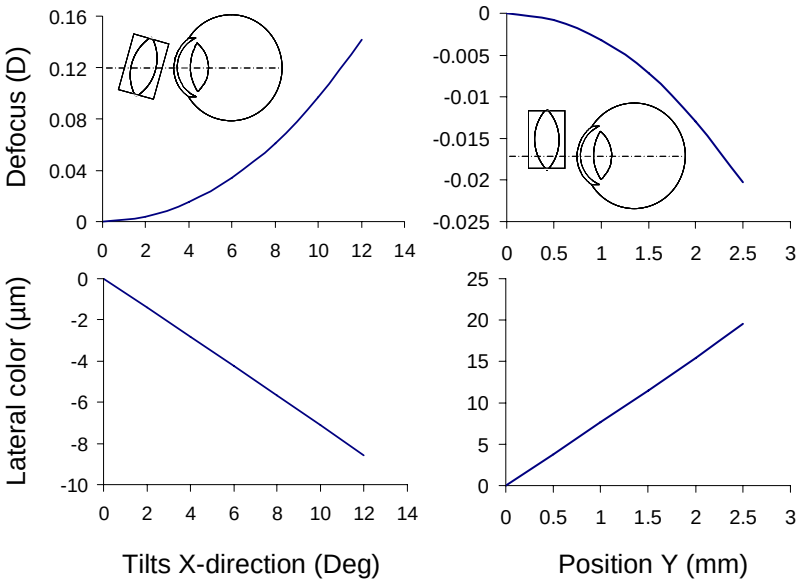

Fig. 4. Tolerance of the achromatizing lens to tilts (left column) and to off-axis centering (right side of the figure). The change of defocus and the lateral color are presented in both cases as a function of the tilt and the displacement, in degrees and in millimeters, respectively.

#69489 - $15.00 USD Received 30 March 2006; revised 14 June 2006; accepted 19 June 2006

Another potential source of errors is the incorrect centering of the AL. Assuming there are not tilts, the AL could be still misaligned with respect to the eye's entrance pupil. The right side of Fig. 4 shows the corresponding results for this particular situation. At the top of the figure the defocus is presented as a function of the displacement of the lens from the center along the Y axis. The symmetry of the problem assures similar results, in absolute values, if the X axis would be considered. As expected, the error in this case is smaller, an order of magnitude below the case of tilts. The small variations in defocus found, even for rather noticeable misalignments like 2 mm (which actually is a very severe value accounting for the fact that the studied pupil is 6 mm diameter), indicates that the AL does not introduce spherical aberration. In total absence of spherical aberration defocus error should be strictly zero. As in the case of tilts, lateral color is also presented at the bottom as a function of the change in position. In this situation, the calculations show that lateral color is increasing with the error in the centering of the AL. Although the increase for the studied range is more important here as compared to the case of tilts, the lateral color is still within reasonable values.

In the next section, the results obtained with and without the AL in real eyes will be presented.

3.2. Measurements in real eyes

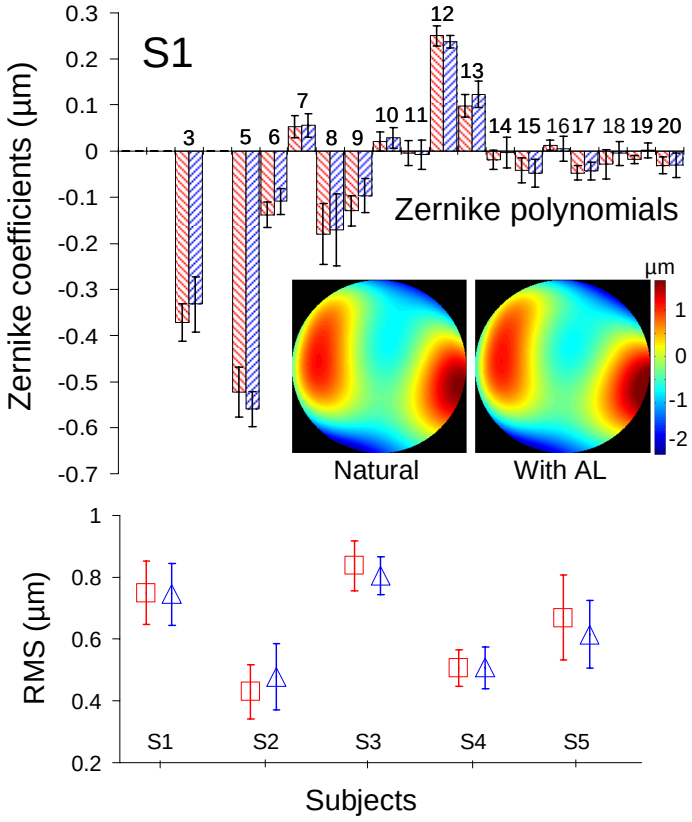

Fig. 5. Top: average ocular aberrations (Zernike polynomials, 6 mm diameter), across all 60 samples and all wavelengths, for subject S1 with and without AL (red and blue color, respectively). Error bars correspond to the standard deviation. Bottom: root mean square (RMS) of the wavefront aberration for each subject with and without the AL (red and blue color, respectively).

#69489 - $15.00 USD Received 30 March 2006; revised 14 June 2006; accepted 19 June 2006

Ocular aberrations were obtained by using the Hartmann-Shack wavefront sensor in 5 different subjects, with and without the AL. The eye model used in this work has been also employed in the study of off-axis monochromatic aberrations [48]. However human eye monochromatic aberrations differ across subjects. Consequently, measurements in real eyes are advantageous, since they also include the possible misalignments present in the system. Ocular aberrations with and without the AL lens were obtained in terms of the Zernike polynomial expansion (OSA standard ordering). At the top of Fig. 5 the coefficients of the wavefront up to the fifth order are presented for one of the subjects (S1), obtained through a pupil of 6 mm diameter. Tilts and defocus are not showed in the figure. Actually, the wavefront sensor cannot retrieve absolute tilts, since they are inherently affected by the entrance angle of the illuminating beam in the eye. The Zernike coefficients were obtained as the average values from all the measurements performed under each of the interference filters. Changes in aberrations other than defocus are within experimental error, and thus we averaged across wavelengths [25]. In Fig. 5 the red color indicates the measurements with the AL while blue color corresponds to the natural aberrations of the subject. Error bars show the standard deviation for every Zernike coefficient. The figure shows that the aberrations obtained with and without the AL are virtually identical, indicating that the optical quality of the AL is very high. Even high order polynomials exhibit this trend. The small variations presented in certain Zernike terms, as those found in the astigmatism (polynomials number 3 and 5) are covered by the corresponding error bars, indicating that the differences are not statistically significant. The spherical aberration, Zernike polynomial number 12, is also similar with and without the AL, corroborating the results obtained with the eye model. The wave aberration, excluding defocus and tilts, for this particular subject is also depicted in Fig. 5, qualitatively showing the virtually null effect of the AL on the optical quality of the eye. The rest of the subjects presented a similar behavior, showing practically identical monochromatic aberrations with and without the AL. At the bottom of Fig. 5 the root mean square (RMS) of the wavefront for every measured subject is depicted, in red color for the case of AL and in blue for the natural aberrations of the eye. In all the subjects the RMS with and without the AL is analogous, being the small differences found in some subjects within the range of the error bars.

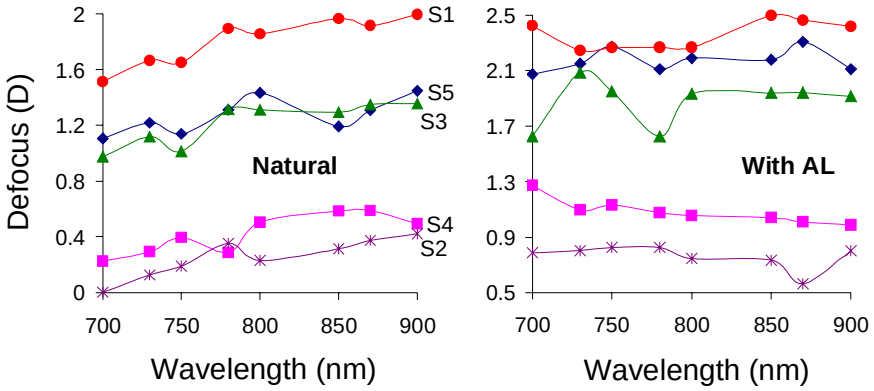

Fig. 6. Defocus obtained in the NIR for each subject, presented with different colors and symbols, without and with the achromatizing lens (left and right side, respectively).

Defocus was the only term presenting a significant variation in the experiment. As an average value, LCA in the human eye, from 700 to 900 nm, is known to originate a change of 0.4 D [25]. The obtained results for the defocus in each subject are presented in Fig. 6. On the left side of the figure the defocus in the natural case is showed as a function of the wavelength. Because of individual differences in the refraction, the curves of every subject appear shifted with respect to the others. The size of the symbols covers in most of the cases

#69489 - $15.00 USD Received 30 March 2006; revised 14 June 2006; accepted 19 June 2006

the standard deviation of the presented average defocus at each wavelength, obtained from two consecutive runs (both accomplished in ~ 5 sec). At the right of the figure the defocus obtained when implementing the AL in the system is depicted, following the same color code used at the top for each subject. In this last case, by using the AL the increase of the defocus with wavelength is not as evident, showing in some cases a flatter evolution across different wavelengths. The AL introduces a theoretical change in the defocus at 800 nm of 0.66 D, making the eye slightly myopic. The average value obtained from the measured subjects was 0.55 ± 0.23 D. In the figure, some points corresponding to the shorter wavelengths in subject 3 show a change close to 0.4 D. These jumps are also present in other subjects, although their magnitude is notably smaller. These variations are believed to be due to experimental errors mainly produced by changes in accommodation during the measurements in some subjects. Accommodation was initially paralyzed for the experiment, but the capability of the eye to restore accommodation exhibits huge differences among individuals. Moreover, accommodation is never totally paralyzed, even under the effect of cyclopentolate. Other source of variation for the defocus during the measurements was the possible change in the relative tilt between the AL and the eye's entrance pupil, whose effects have been already presented in this section with the eye model.

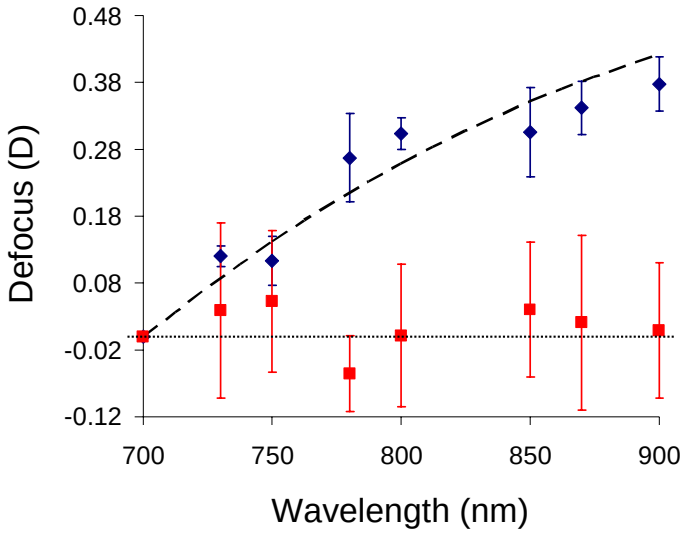

Fig. 7. Average defocus in the NIR obtained from five subjects with and without the achromatizing lens (red and blur color, respectively). Error bars show the standard deviation. All data are shifted to the reference wavelength 700 nm. The dashed line shows the evolution of the defocus predicted by the eye model. The dotted line indicates the zero defocus value.

The average results from all the subjects obtained for the defocus are presented in Fig. 7. In order to perform the average, all the data were shifted so that the origin of defocus was taken at 700 nm. The error bars show the standard deviation. The red color shows the effect of the AL and the blue corresponds to the natural defocus, the LCA. The dashed line is the defocus predicted by the Navarro's eye model. The dotted line corresponds to the zero defocus. The figure shows a very good agreement between the model and the experimental data, which also reproduce the LCA found in previous studies [25]. The error bars are small, therefore indicating that, despite the possible experimental errors already mentioned, the LCA was similar in all the subjects. The figure also shows that the AL makes the LCA virtually zero in the considered range. All the experimental points are located close to the zero defocus line, with their respective error bars overlapping this value. The magnitude of the error bars is

#69489 - $15.00 USD Received 30 March 2006; revised 14 June 2006; accepted 19 June 2006

slightly larger in this case as compared to the natural LCA. This could be explained in terms of the additional source of error introduced by the possible tilts between the eye's pupil and the AL, as it has already been mentioned.

4. Discussion and conclusions

The mathematical calculations and experimental results presented in this work show that the proposed AL corrects the average LCA of the human eye in the NIR (from 700 to 900 nm), leaving the rest of the aberrations practically unaffected.

Individual deviations have been also reported across subjects in the LCA correction. Fixating stimulus was not used during the measurements, introducing an additional source of error. Due to the use of monochromatic near infrared light (from 700 to 900 nm), subjects perceived the illuminating beacon as a rather dim stimulus. Therefore it barely provokes accommodation response. Since we used cyclopentolate, we assumed accommodation would be paralyzed during measurements, which was not the case in some subjects, as Fig. 6 shows. The use of a fixation target might have had an impact in the stability of the measured ocular aberrations in some cases, reducing the variability in the chromatic aberration across subjects. It should be noticed that the use of visible stimulus requires the compensation of the existing chromatic aberration between near infrared and visible wavelengths.

The design of the AL is relatively simple, based on a triplet using only regular optical glasses combined symmetrically, making a cost-effective and easy to implement lens. Extended range of use for the AL was also explored in the simulations, from 600 to 1000 nm, showing a ~ 90 % reduction in the chromatic focal shift at the retina (321.13 μm in the natural eye and 39.67 μm using the AL). Although the eye model nicely predicts the behavior of the human eye in the visible and near IR, there are no experimental measurements of ocular aberrations beyond 900 nm supporting the use of the model up to 1000 nm. Consequently, these results on the performance of the AL covering a spectral bandwidth of 400 nm should be taken as preliminary ones, to be experimentally confirmed in the future.

The AL has been designed to be conjugate with the eye's entrance pupil, with a magnification of ± 1. The lens can be also placed directly in front of the eye, close to the cornea. We have obtained similar performance in the correction of the LCA, within 85 %, with distances of up to 30 mm from the cornea. This way simplifies the optical system, although it might not be convenient for retinal imaging as it will be discussed latter in this section.

The calculations presented in Fig. 4 show that there is a change in defocus as a function of tilt. This can be possibly reduced by using a more compact design, making the AL thinner, although in this case more exotic materials would be required, incrementing the cost of the lens. The tolerance of the AL to misalignments in both tilts and displacements in the transverse plane, when the lens is intended to be used in normal incidence, is quite high. The simulations presented in Fig. 4 have demonstrated that lateral color appears as a consequence of existing misalignments, although errors in centering the AL contribute more than those produced by tilts. In practice, it is relatively easy to assure a good matching between pupils, while the correct tilt is more difficult to achieve. In addition, calculation and real measurements have demonstrated that the amount of spherical aberration introduced by the proposed AL is negligible.

The designed AL can be used for retinal imaging purposes. In particular, the AL is especially suitable for those ophthalmoscopes whose retinal images are obtained by scanning the illuminating beam onto the retina, as scanning laser ophthalmoscopes (SLO), including the confocal version, and primarily in the majority of the optical coherence tomography (OCT) apparatus. In SLO, the use of polychromatic light might reduce the speckle typically generated with light of high coherence, increasing the signal-to-noise ratio. In OCT the use of polychromatic light sources is mandatory, therefore the use of the AL is more suitable for this latter modality. Moreover, in OCT the spectral bandwidth of the light source governs the axial resolution, making the use of a broad spectrum very convenient. Regarding transverse resolution, in a previous study [39], we found that the correction of the chromatic aberration

#69489 - $15.00 USD Received 30 March 2006; revised 14 June 2006; accepted 19 June 2006

also allows for better transverse resolution, because an associated improvement in the contrast of the retinal images. Calculations were performed for the case of a fiber-based setup, where confocal detection can be assumed. In other cases, the effective polychromatic PSF is different and the results might not be applicable. Due to the complexity of the problem, rigorous calculations on transverse resolution improvement should be performed for each specific case, incorporating the particular characteristics of the optical system in order to properly model the effective polychromatic PSF.

For both SLO and OCT we propose the use of the AL conjugated with the eye's entrance pupil, leaving the scanning system between the eye and the AL. This configuration makes that both the illuminating beam as the light reflected by the retina pass through the AL with normal incidence, avoiding the possible lateral color introduced by the AL when using a tilted beam. This is precisely the case we have studied along the present work. The LCA of the eye is practically constant for small and moderate fields [20], so the effect of the AL should still benefit the retinal images obtained in these ranges. In addition, the proposed practical implementation of the AL maintains the lateral color unaffected, being only produced by the patient's eye [4].

Another advantage of the studied AL is that monochromatic aberrations, excluding defocus, are not affected by using the AL (presented in Fig. 5), which is of a huge practical importance for a hypothetical correction of these aberrations by using adaptive optics (AO). In both standard OCT [35,36] and UHR OCT [37,38], AO has been demonstrated for increasing the transverse resolution, revealing intraretinal features in the living retina otherwise undetectable. The implementation of the AL in such AO system might produce a full correction of the ocular aberrations; it could perhaps be named *pancorrection*, using the Greek prefix pan- meaning all, with an extended benefit on the retinal images' quality. The use of the AL could also solve the apparent paradox occurring in AO UHR OCT when correcting the monochromatic aberrations in large pupils [38], probably related to the chromatic aberration of the eye [39], and already mentioned in the introduction of this work.

Acknowledgments

The authors gratefully acknowledge B. Hofer and P. Qiu, Medical University of Vienna, for their kind help serving as subjects in the experiment.

This research was supported by FWF Y159-PAT, the Christian Doppler Society, FEMTOLASERS Produktions GmbH, and Carl Zeiss Meditec AG.

W. Drexler, the corresponding author, can be reached by phone, 43-1-4277 60726; fax: 43-1-4277 9607; or e-mail, wolfgang.drexler@meduniwien.ac.at.

#69489 - $15.00 USD Received 30 March 2006; revised 14 June 2006; accepted 19 June 2006